A STUDY OF 0°-FIBRE MICROBUCKLING IN MULTIDIRECTIONAL COMPOSITE LAMINATES

P. Berbinau and C. Soutis

Department of Aeronautics, Imperial College of Science, Technology & Medicine
Prince Consort Rd, London SW7 2BY, UK

SUMMARY: The aim of this work is to study the compression failure mechanisms in multi-directional CFRP composite laminates with internal 0°-plies. In such laminates, as in uni-directional 0° laminates, catastrophic failure initiates by kinking of 0°-plies at the free-edges or manufacturing defects. T800/924C carbon fibre-epoxy laminates with a $[(\pm\theta/0_2)_2]_s$ lay-up with θ equal to 30°,45°,60° or 75° are used here to study the effect of the supporting ply angle θ on the stress initiation of 0°-fibre microbuckling. Experimental compressive strengths are compared to theoretical predictions obtained from a fibre kinking model that incorporates interlaminar shear stresses developed at the free edges at $(0/\theta)$ interfaces. Initial misalignment of the fibres and non-linear shear behaviour of the matrix are also included in the analysis. Interlaminar stresses do not appear to have a significant influence on fibre microbuckling initiation and on the static compressive strength of the laminates.

KEYWORDS: composite laminates, compression, microbuckling, kink bands, interlaminar edge stresses, compressive strength.

INTRODUCTION

The compressive strength of long, aligned fibre composites may be as low as 60% of their tensile strengths [1-4], thus it is recognised that the compressive strength is often a design limiting parameter. An understanding of the compression failure modes is therefore crucial to the development of improved composite materials. The critical mechanism in the compressive fracture of unidirectional polymer matrix composite laminates is plastic microbuckling [5], with creation of a kink band. In carbon fibre-epoxy systems the kink band width is typically of the order of ten to fifteen fibre diameters, and is inclined at an angle β=15-30° to the y-axis orthogonal to the loading x-axis. The through-thickness axis is z.

Unidirectional composite laminates are rarely used in structural components but are usually combined with plies of varying orientation in a multidirectional laminate. However, it is the 0° layers in such a laminate that carry most of the applied load, and, from a structural-design viewpoint, it is important to know the failure stress of these plies and how it relates to the stress of the unidirectional laminate on its own. In this paper the effect of the supporting ply orientation on fibre microbuckling initiation and final failure of $[(\pm\theta/0_2)_2]_s$ T800/924C carbon

fibre-epoxy laminates is examined, with ±θ equal to either ±30°, ±45°, ±60° or ±75° (labelled L30, L45, L60 and L75, respectively). This particular lay-up has been selected to study more methodically the effects of the local constraint (supporting ply orientation) on fibre microbuckling initiation. The interlaminar shear stresses developed at the laminate free edge, between the 0° plies and the adjacent off-axis plies, are determined and incorporated into a fibre kinking model reported previously [6, 7]. The model is based on an initially misaligned fibre bundle on a non-linear foundation (resin) that is capable of finite deflections. Analytical compressive strength predictions are compared with experimental measurements.

EXPERIMENTS

All laminates were autoclaved from Toray T800 carbon fibres pre-impregnated with Hexcel Composites BSL 924C epoxy resin. The laminates were later inspected ultrasonically to confirm specimen quality. The unidirectional specimens (labelled L0) were of gauge section 10mm x 10mm; this gauge length is sufficiently short for anti-buckling guides not to be required. They were tested in compression using a modified Celanese test rig [8, 9]. The multi-directional specimens $[(\pm\theta/0_2)_2]_s$ (see Table 1) were of gauge section 116 mm x 30 mm,

Table 1: Average compressive strength properties of T800/924C $[(\pm\theta/0_2)_2]_s$ plates

Laminate	Angle θ	E_{xx} (GPa)	G_{xy} (GPa)	σ_f (plate) (MPa)	ε_f (%)	σ_f (0°-ply) (MPa)
L0	0°	160	6.0	1430	1.1	1430
L30	30°	103 *(112)*	*(19.2)*	832 *(995)*	0.88	1178
L45	45°	81 *(92)*	*(23.6)*	745 *(820)*	0.95	1298
L60	60°	83 (87)	*(19.2)*	660 *(768)*	0.93	1230
L75	75°	81 *(86)*	*(10.4)*	653 *(757)*	0.89	1233

Notes: ( ) Predicted values, assuming elastic LPT and max stress criterion

and were tested using an anti-buckling device to prevent bending during the test. All specimens were end-tabbed with glass/epoxy, and had strain gauges bonded on both faces. Compression tests were conducted in a screw-driven test machine at a displacement rate of 0.017 mm·s^{-1}. Full details on the experimental technique are given by Soutis [9].

Compressive strength data

The stress-strain response of the T800/924C unidirectional $[0_8]_s$ laminate is linear almost up to failure, with an elastic modulus E=160 GPa, a failure stress σ=1480-1600 MPa, and an average failure strain ε_f=-1% [1, 3]. In comparison, the average tensile strength for this material is 2400 MPa, and a failure strain close to 1.8%. Post failure examination of the fracture surfaces using a scanning electron microscope revealed that failure is by fibre kinking. The kink band angle β is approximately 15°. The fibre orientation angle (from their initial direction, x) within the band is ϕ=30°, and the kink band width is W=50-60μm, approximately equal to ten fibre diameters (d=5.5μm). Failure of the $[(\pm\theta/0_2)_2]_s$ laminates is sudden and mainly occurs within the gauge length; some specimens failed near the grip (due to stress concentrations induced by the clamping forces) but results from these tests were discarded. The longitudinal strain on the two faces of the specimen is initially the same, but as the applied load is increased the strains usually diverge, indicating bending. Final fracture involves splitting parallel to the fibres, delamination between the 0° and the θ plies and fibre

microbuckling. Fibre microbuckling in the 0° layers is considered as the critical-damage mechanism, which causes catastrophic fracture of the specimen. The investigation of ply-interaction phenomena by fractographic methods is very difficult because of the extensive post-failure damage. Results for the average failure stress for all successfully tested specimens are presented in Fig. 1. They show that the failure stress increases as the supporting

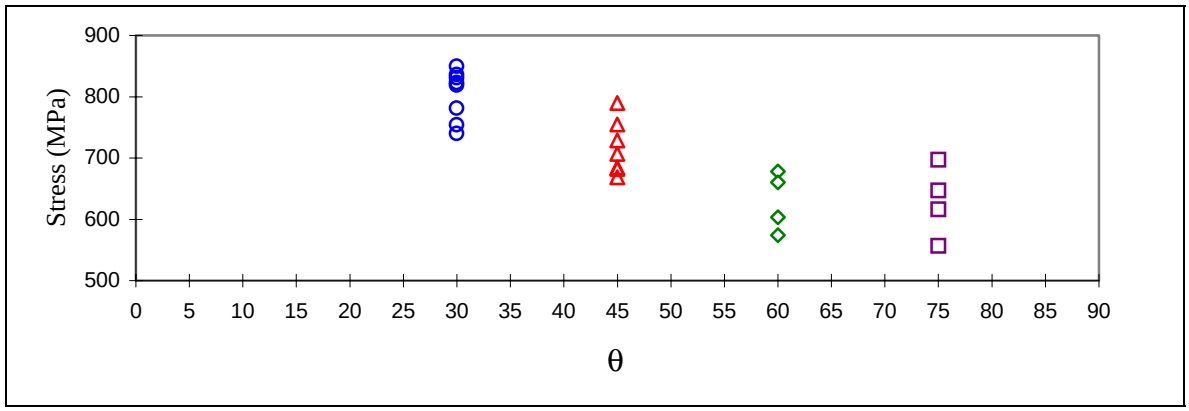

Fig. 1: Experimental failure stress for laminates $[(\pm\theta/0_2)_2]_s$

ply orientation θ is reduced. At small angles the fibres are more aligned in the loading direction and offer higher bending resistance to the load. The failure stress is maximum at 1430 MPa [3] for a 100% 0° laminate. Using the laminate plate theory and the measured laminate strength, the maximum stress developed in the 0° plies within the multidirectional laminate was found to be up to 17% lower than the stress in the unidirectional 0°-laminate (Table 1). The lowest drop is 5% for θ=45°, suggesting that for θ=45° the lateral support to the axial layers and the resistance to fibre microbuckling is optimum. The theoretical strengths for the $[(\pm\theta/0_2)_2]_s$ laminates, predicted by the LPT and the maximum stress failure criterion are higher (10-17%) than the measured values because the strain in the composite is assumed uniform and the response linear elastic to failure (Table 1).

In the following section, the ply interaction is analysed in terms of interlaminar shear stresses that develop at the ply interface. These stresses are then implemented in a recently developed fibre buckling model [6] that accounts for matrix non-linearities to estimate the failure stress of the 0°-ply and then determine the unnotched compressive strength of the various T800/924C $[(\pm\theta/0_2)_2]_s$ laminates examined in this investigation.

COMPRESSIVE STRENGTH PREDICTION

The experimental work presented above shows that in multidirectional laminates dominated by internal 0° plies, failure occurs by in-plane microbuckling, and that the stress (or strain) level at which 0° fibre microbuckling initiates is influenced by the initial fibre waviness, the non-linear resin shear constitutive behaviour, and the orientation of the supporting plies adjacent to the 0° layers. This is in agreement with results published earlier by other workers (see for instance Guynn *et al* [10]). On the other hand, in laminates were the surface plies are 0°-plies, or in cross-ply laminates, failure occurs rather by out-of-plane microbuckling [11].

The classical laminate plate theory [12] assumes that the state of stress within each lamina of a multidirectional laminate is planar. This assumption is not true in the vicinity of the free

edge. Owing to stiffness discontinuities between plies of different orientation, large interlaminar (through-thickness) stresses exist near the traction free-edge regions in multi-directional composite panels (see for instance Pipes, Pagano [13]). Since 0° fibre micro-buckling initiates from the specimen free edge, where the fibre support is substantially reduced (as confirmed by experiments [10]), it becomes very important in the strength prediction of 0°-dominated laminates to estimate the through-thickness edge stresses and include their influence on the stability of the 0° layers. This concept was put forward for the first time by Berbinau [6], who further showed that among the interlaminar stresses σ_z , τ_{zy} and τ_{zx} , only the shear stress components (τ_{zy} , τ_{zx}) are likely to influence the in-plane movement of the 0° fibres. The stacking sequence of the laminate was chosen so that σ_z under compressive loading was compressive, making therefore no contribution to edge delamination or 0° fibre (in-plane) microbuckling. It should be noted that although some existing models [14,15] included through-thickness stresses, they did not incorporate explicitly interlaminar free-edge stresses nor studied their effect on the in-plane microbuckling of 0° fibres.

Briefly, the general structure of the Berbinau and Wolff theoretical approach [6,7] is to calculate first the interlaminar shear stresses τ_{zy} and τ_{zx} , here by using the Puppo & Evensen model [16]. Then the shear stresses are incorporated into a general microbuckling equation [6, 7] for a 0° fibre located at the specimen free-edge in a 0°-ply; equilibrium conditions are applied to relate the compression load to the deformation of the 0° fibres and obtain the 0°-ply failure stress. Finally, this value is used with the maximum stress failure criterion to predict the laminate compressive strength. In the present paper, the non-linear matrix response is considered by expressing the composite shear modulus as a function of shear strain, G(γ).

Influence of interlaminar stresses

The interlaminar stresses arising during the compression loading of a $[(\pm\theta/0_2)_2]_s$ laminate are calculated by the Puppo & Evensen method [16] extended to laminates with an arbitrary number of layers [6]. A program was written using the *Mathematica* software [17] for this purpose. Results are presented in Fig. 2(a), where the maximum values of the interlaminar

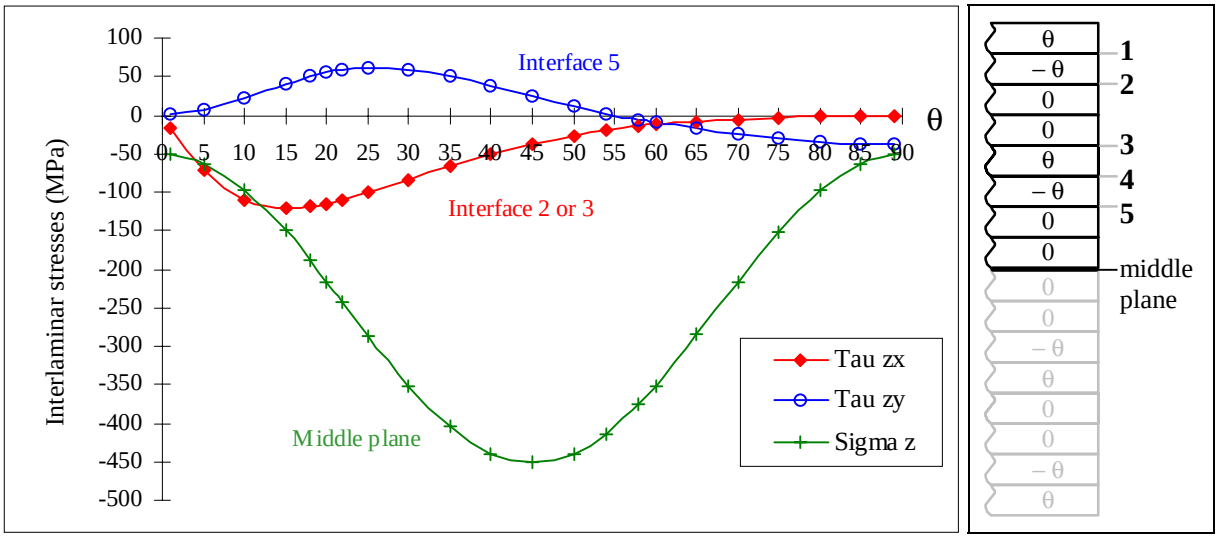

(a) (b)

Fig. 2: (a) Maximum interlaminar edge stresses (strain =-1%). (b) Interface numbering

stresses are plotted as a function of the orientation θ of the supporting plies. The ply interface where a given stress reaches its maximum value, is also indicated. Interfaces are numbered as in Fig. 2(b), starting from a surface ply. For θ between 60° and 65° both shear stress components are very small, suggesting that the instability effect on the neighbouring 0° layers is not significant. The stress magnitude is directly proportional to the applied compressive strain ε_f. The stress results presented in Fig. 2(a) correspond to ε_f =-1%, which is close to the failure strain measured for the T800/924C laminates, Table 1. The normal stress σ_z has been determined by using the approximate solution of Pipes and Pagano [18]. Delamination initiation at the free edge can then be predicted by using the Tsai-Wu quadratic failure criterion [12, 19],

$$\sqrt{\tau_{zx}^2 + \tau_{zy}^2} = \tau_{IL} \qquad (1)$$

where τ_{IL} is the interlaminar shear strength of the composite (ILSS=105 MPa).
For $10° \le \theta \le 25°$, edge delamination is expected to occur, as shown on Fig. 3, at an applied compressive strain of $0.95\% < \varepsilon_f < 0.88\%$.

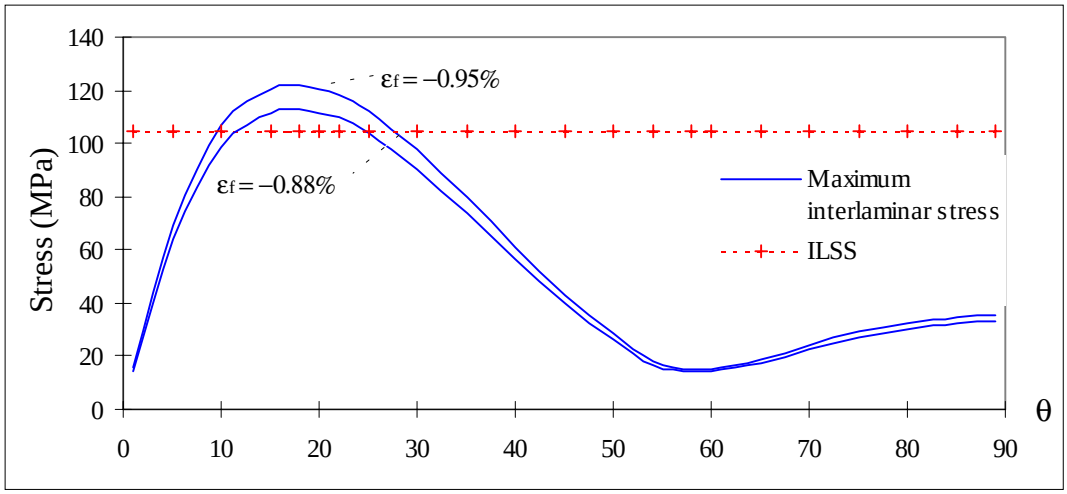

Fig. 3: Delamination criterion for an applied compressive strain between 0.88% and 0.95%

0°-fibre microbuckling model

The next step in the present strength prediction is to incorporate the interlaminar shear stresses into a general microbuckling equation for a 0°-fibre (modelled as a Euler beam on a non-linear foundation). In order to predict the onset of fibre microbuckling, it is convenient to model the initial fibre waviness by a sine function $v_0(x)$ of amplitude V_0 and half-wavelength λ_0. Under the influence of the applied compressive stress, the sine function $v_0(x)$ will deform into a new sine wave function $v(x)$ of amplitude V and half-wavelength λ. We thus have:

$$v_0(x) = V_0 \cdot \sin\left(\frac{\pi x}{\lambda_0}\right) \qquad \text{and} \qquad v(x) = V \cdot \sin\left(\frac{\pi x}{\lambda}\right) \qquad (2)$$

Assuming small deflections and a constant axial force P, the equilibrium equation of the deflected fibre is [20, 21]:

$$E_f I \frac{d^4(v - v_0)}{dx^4} + P\frac{d^2 v}{dx^2} + p - A_f G(\gamma)\frac{d^2(v - v_0)}{dx^2} = 0 \qquad (3)$$

where E_f , A_f , and I are the fibre modulus, cross-section area and second moment of inertia, respectively. p is the distributed transverse force normal to the fibre, Fig. 4©. Several researchers have developed microbuckling models with various expressions for p (see for instance [14, 20, 22-24], and also [2] for a comprehensive review on this topic). In Eqn 3, the composite shear modulus G is not constant but is a function of the shear strain γ. That means that the non-linear shear response of the composite system is fully considered in the model. For the T800/924C system the shear stress-strain curve τ(γ) has been experimentally determined [3] and can be very well approximated (see [21]) by:

$$\tau(\gamma) = \tau_{ult}\left(1 - \mathrm{Exp}\left(-\frac{G_{12}\,\gamma}{\tau_{ult}}\right)\right) \tag{4}$$

Eqn 4 is used to derive an analytical expression for the slope G(γ) of the τ–γ curve, which appears in the differential equation (3). For the T800/924C system, the ultimate shear stress τ_{ult} is found experimentally to be 108 MPa and the elastic shear modulus G_{12} is 6 GPa.

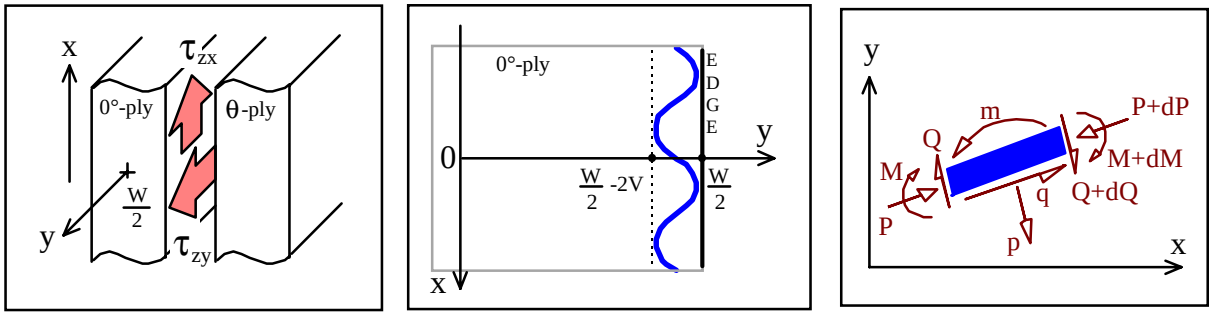

(a) (b) (c)

Fig. 4: (a) Interlaminar shear stresses. (b) Edge fibre in a 0°-ply. (c) FBD for a fibre.

In the current work, p is expressed in terms of the interlaminar shear stresses τ_{zx} and τ_{zy} , which influence the stability of the axial plies. Consider an initially wavy fibre located at the edge of the ply (y=W/2), Fig. 4(b). It is subjected to a normal component p and a tangential component q along its length, Fig. 4(c). As a first approximation, for the kinking deformation under consideration, it is plausible to set q=0. The normal component p can be expressed in terms of τ_{zx} and τ_{zy} as:

$$p(s) = d_f\left(\tau_{zx}\,\vec{n}\cdot\vec{i} + \tau_{zy}\,\vec{n}\cdot\vec{j}\right) \tag{5}$$

where d_f is the fibre diameter, $\vec{n}$ is the unit normal to the fibre, $\vec{i}$ and $\vec{j}$ are the unit vectors in the x and y directions, respectively. Due to symmetry, only a fibre wavelength needs to be considered. The orientation of the normal $\vec{n}$ varies along the fibre length. It can be shown (see Berbinau *et al* [21]) that for a V value small compared to λ, the τ_{zx} component in Eqn 5 can be neglected, and the normal stress p experienced by a fibre at the edge can be approximated by:

$$p(v) = d_f\left\{\tau_{zy}\Big|_{\frac{W}{2}-2V} - \tau_{zy}\Big|_{\frac{W}{2}}\right\} \approx -2\,d_f\cdot\left\{\left[\frac{d\tau_{zy}}{dy}\right]_{\frac{W}{2}}\right\}\cdot v \tag{6}$$

The shear strain γ can be approximated by the slope of the curve $(v\text{-}v_0)(x)$. The applied load

P on a fibre can be expressed in terms of the stress σ_0 developed on the 0°-ply, the fibre cross-section area A_f and the fibre volume fraction V_f. We have:

$$\gamma \approx \frac{d(v - v_0)}{dx} \qquad \text{and} \qquad P \approx \frac{A_f}{V_f}(\sigma_0) \tag{7}$$

Substituting equations 6 and 7 into Eqn 3 yields the following differential equation:

$$E_f I \frac{d^4(v - v_0)}{dx^4} + \frac{A_f \sigma_{0^\circ - ply}}{V_f} \cdot \frac{d^2 v}{dx^2} - 2 d_f \left\{ \left[\frac{d\tau_{zy}}{dy} \right]_{\frac{w}{2}} \right\} \cdot v - A_f G \left(\frac{d(v - v_0)}{dx} \right) \cdot \frac{d^2(v - v_0)}{dx^2} = 0 \tag{8}$$

Eqn 8 is non linear and gives the compressive stress σ_0 in the 0° ply in terms of the maximum amplitude V of the 0° buckled fibre, fibre properties and interlaminar shear stress τ_{zy}.

Strength results

In the current analysis, Eqn 8 is solved numerically by using the *Mathematica* software [17]. The input data required are the fibre diameter d_f, fibre volume fraction V_f, the interlaminar shear stress τ_{zy}, the non-linear shear response, and the initial fibre amplitude V_0, which is calculated from the microbuckling half-wavelength λ_0 and the initial misalignment angle ϕ_0. The initial fibre waviness may be measured from a microscopic observation of the 0°-ply; for the T800/924C system ϕ_0 was found equal to ≈2° [1-4]. The half-wavelength λ_0 is of the order of 10-15 fibre diameters [1-4]. In Fig. 5, the maximum fibre amplitude, V, versus 0°-ply stress is presented for a T800/924C $[(\pm 30/0_2)_2]_s$ laminate. V increases slowly with increasing applied stress σ_0 and then grows dramatically fast. Failure of the 0° ply due to fibre

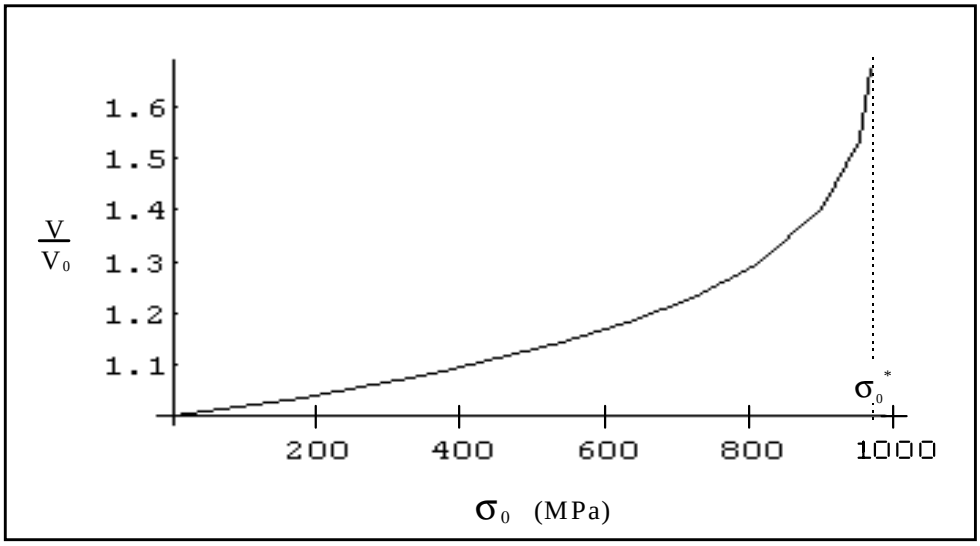

Fig. 5: Microbuckling amplitude V vs. the stress σ_0 on a 0°-ply ($[(30/-30/0_2)_2]_s$ laminate).

microbuckling occurs when the fibre amplitude V starts to increase asymptotically, Fig. 5. For θ=30°, the critical stress σ_o^* is 961 MPa compared to 1178 MPa, estimated from the measured strength data and the laminate plate theory. For a 100% 0° laminate and $\lambda = 10 \cdot d_f$, Eqn 8 predicts σ_o^* =968 MPa, 30% lower than the average experimental strength. It should be noted

that σ_o^* is strictly the critical stress at which fibre microbuckling initiates and not final failure stress. However, since final failure is considered as initiation controlled rather than propagation, σ_o^* could be taken as the 0°-ply strength within the multidirectional laminate, which here appears to be a conservative estimate. In Table 2 the 0°-ply critical stress is presented for different θ (orientation of the supporting plies) and λ (fibre waviness) values. It can be seen that the interlaminar shear stress has a small influence on the strength of the 0°-ply and is almost independent of the off-axis orientation θ. This is in good agreement with previous [9, 10] and present experimental evidence. Hence the off-axis plies orientation angle seems to have a small influence on the 0° fibre microbuckling initiation stress (or strain); the initial fibre waviness and non-linear shear response are more important parameters.

Table 2: Predicted failure stress σ_0^* of the 0°-ply in MPa, Eqn 8.

Off-axis ply orientation, θ°	Fibre wavelength $\lambda=10\cdot d_f$	$\lambda=15\cdot d_f$	$\lambda=20\cdot d_f$
0	968	743	657
30	961	737.5	637
45	961	723	635.5
60	975	748	673
75^+	977	751.5	680
90^+	979	753.5	683.5

Note: $^+$ For θ>70°, out-of-plane fibre microbuckling could occur and a different model is required.

Once the failure stress of the axial ply is known, the compressive strength of the multidirectional laminate can be determined by using the laminate plate theory and the maximum stress failure criterion or simply by the stiffness ratio method, given below:

$$\sigma_{lam} = \frac{\sigma_0^*}{N\,E_{11}} \sum_{k=1}^{N} n^{(k)} \cdot E_{x\theta}^{(k)} \qquad (9)$$

where σ_{Lam} is the laminate strength, σ_o^* is the reduced strength of the 0° lamina, N is the total number of plies in the laminate, E_{11} is the 0° ply stiffness in the fibre direction, n is the number of plies of a given orientation θ and $E_{x\theta}$ the modulus of a θ-ply along the load x-axis.

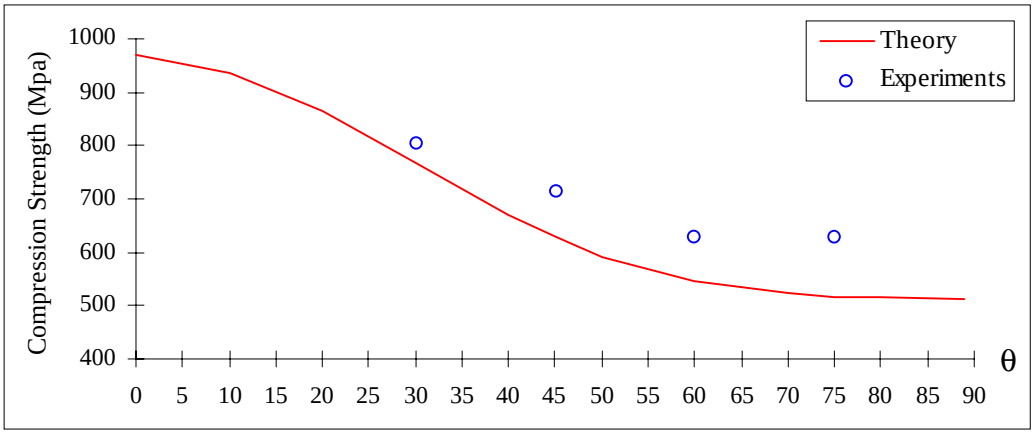

Fig. 6: Comparison of the experimental and theoretical compressive strengths for $[(\pm\theta/0_2)_2]_s$

The calculated 0°-ply strength, σ_o^*, takes into account the ply interaction effect as well as the non linear response of the resin material and the initial fibre waviness. Varying θ from 0° to 90°, the theoretical compressive strength σ_{Lam} as a function of the angle θ for the T800/924C $[(\theta/-\theta/0_2)_2]_s$ laminate is obtained by following the above procedure. The results are summarised in Fig. 6 and compared to experimental strength measurements. The static compressive strength of the $[(\pm 30/0_2)_2]_s$ laminate is higher than the other lay-ups with θ>30° due to higher bending stiffness. However, under fatigue loading the interlaminar shear stresses may introduce edge delamination, Fig. 3, which would reduce the support to the 0° layers, causing fibre microbuckling and premature laminate failure. In this case, the laminate with ±60 off-axis plies is expected to perform better due to lower interlaminar stresses.

CONCLUSIONS

Experiments show that the static compressive failure of unidirectional and multidirectional unnotched $[(\pm\theta/0_2)_2]_s$ T800/924C carbon fibre-epoxy laminates is controlled by 0°-fibre microbuckling. Average failure strains ε_{fav} for each of the four angles θ (30°,45°,60°,75°) examined are scattered between ≈-0.9 % and ≈-1 %. The present tests do not reveal any obvious trend as to the variation of the failure strain with the angle θ, hence the off-axis layers have only a small influence on the compressive failure stress (or strain). Specimens with θ=45° appear to provide better resistance to fibre microbuckling with an average failure strain of -0.95%. The 0°-ply stress in a such laminate is ≈1300 MPa compared to 1430 MPa measured for the 100% 0° laminate. The 10% strength reduction can be due to ply interaction (edge effects) and probably manufacturing defects (interlaminar voids, resin rich regions). Soutis *et al* [8, 9] and Guynn *et al* [10] obtained similar experimental results.

The modified Berbinau-Wolff [6, 7] microbuckling model incorporates the non-linear resin shear response, fibre imperfections (waviness) and fibre content. In the model the effect of the interlaminar shear stress τ_{zy} that develops at the laminate edges is included explicitly to account for ply interaction. It is revealed that the τ_{zy} stress component can damage the stability of the axial plies but the effect of resin softening and fibre waviness are more significant. The instantaneous tangent shear modulus G rather than the elastic modulus controls the fibre microbuckling initiation of initially misaligned fibres. Theoretical predictions are accurate to within 10-15%. It is worth pointing out here that out-of-plane microbuckling is the failure mode for θ=90° [11], and that experiments [25] suggest that it could also be the failure mode for θ > 70°. In fact, the present model hints at such a mode competition, since above θ=60° the τ_{zy} stress can be shown to hinder the in-plane microbuckling of the fibres [6]. Simultaneously, out-of-plane fibre movement is facilitated by the fact that the bending stiffness of the (±θ) plies about the $\vec{y}$ axis decreases as θ increases [25]. Since the present failure model is based on in-plane movement of the 0° fibres, it might not be valid above θ=70°. More experimental observations and theoretical modelling on the failure of $[(\pm\theta/0_2)_2]_s$ laminates with θ>70° are therefore needed. A theoretical and experimental investigation of the influence of the interlaminar stresses near the free edge on 0°-fibre microbuckling initiation under compression-compression fatigue loading will also be of interest. Matrix cracking and edge delamination may then trigger fibre microbuckling at lower applied strains, and the selection of the supporting ply orientation may become more critical than in static loading.

REFERENCES

1. Soutis, C. "Measurement of the Static Compressive Strength of Carbon Fibre-Epoxy Laminates". *Composites Sci. & Techn.*, **42**, 1991, pp.373-392.
2. Schultheisz, R. and Waas, A.M. "Compressive Failure of Composites, Parts I & II". *Progress in Aerospace Science*, **32**, 1996, pp. 1-78
3. Soutis, C. "Compressive Strength of Unidirectional Composites: Measurement and Predictions". *ASTM STP 1242*, (1997) pp.168-176
4. Soutis, C. and Turkmen, D. "Moisture and Temperature Effects of the Compressive Failure of CFRP Unidirectional Laminates". *J. Comp. Mater.*, **31**(8), 1997, pp.832-849.
5. Slaughter, W.S., Fleck, N.A., Budiansky, B. "Microbuckling of Fibre Composites: The Roles of Multi-Axial Loading and Creep". *J Eng. Mater. & Techn.*, **115**(3), 1993, pp.308-313.
6. Berbinau, P. "A Study of Compression Loading of Composite Laminates". *Ph.D. Thesis*, Oregon State University (1997).
7. Berbinau, P. and Wolff, E. "Analytical Model for Prediction of Microbuckling Initiation in Composite Laminates". *ICCM 11*, Gold Coast, Queensland, Australia, July 1997.
8. Soutis, C., Fleck, N.A. and Curtis, P.T. "Compressive Failure of Notched Carbon Fibre Composites". Proc. R. Soc. Lond. A, **440**, 1993, pp.303-312.
9. Soutis, C. "Failure of Notched CFRP Laminates due to Fibre Microbuckling: A Topical Review". *J. Mech. Behav. Mater*., **6**(4), 1996, pp.309-330.
10. Guynn, E.G., Bradley, W.L. and Ochoa, O.O. " A Parametric Study of Variables that Affect Fibre Microbuckling Initiation in Composite Laminates: Part 2–Experiments, *J. Comp. Mater.*, **26** , 1992, pp. 1617-1627.
11. Kominar V. et al, "Compressive Strength of Unidirectional and Crossply Carbon Fibre/PEEK Composites". *J. Mater. Sci*., **30**, 1995, p.2620
12. Jones, R.M. "Mechanics of Composite Materials". Taylor & Francis, 1975.
13. Pipes, R. and Pagano, N. "Interlaminar Stresses in Composite Laminates under Uniform Axial Extension". *J. Comp. Mat*, **4**, 1970, p.538.
14. Swanson, S.R. "A Micro-Mechanics Model for In-Situ Compression Strength of Fibre Composite Laminates". *J. Eng. Mater. & Techn.*, **114**, 1992, pp. 8-12.
15. Shuart, M.J. "Short-Wavelength Buckling and Shear Failures for Compression-Loaded Composite Laminates". *NASA Technical Memorandum 87640*, 1985.
16. Puppo A. H., Evensen H. A. "Interlaminar Shear in Laminated Composites under Generalised Plane Stress". *J. Comp. Mater.*, **4**, 1970, p.204.
17. Wolfram S., "Mathematica", Addison-Wesley, 1993.
18. Pagano, N. and Pipes, R. "Some Observations on the Interlaminar Strength of Composite Laminates". *Int. J. Mechanical Science*, **15**, 1973, pp.679-688.
19. Hu, F.Z., Soutis, C. and Edge, E.C. "Interlaminar Stresses in Composite Laminates with a Circular Hole". *Composite Structures*, **37**, 1997, pp.223-232.
20. Hahn, H. and Williams, J. "Compression Failure Mechanisms in Unidirectional Composites". *ASTM STP 893*, 1986, pp. 115-139.
21. Berbinau, P., Soutis, C., Goutas, P., Curtis, P., "Effect of Off-Axis Ply Orientation on 0°-Fiber Microbuckling". To be published in *Composites - Part A*, 1999.
22. Steif, P., "A Model for Kinking in Fibre Composites - I. Fibre Breakage via Micro-Buckling", *Int. J. Solids & Structures*, **26**, n°5-6, 1990, pp.549-561
23. Hahn, H. "Analysis of kink band formation under compression", ICCM 6, **1**, 1987, p.269
24. Chung, I. and Y. Weitsman, Y. "A Mechanics Model for the Compressive Response of Fibre Reinforced Composites". *Int. J. Solids & Structures*, **31** (18), 1994, pp.2519-1536.
25. Berbinau, P., and Wolff E.G., "Compression of 0°-Ply/Acrylic Sandwich". Submitted for publication in *J. Mater. Sci.*, December 1998.